Finger Force Prediction from Spinal Signals: Machine Learning Pipeline for the Neural Drive

Renato Mio
Chair of Digital Health & Data Science
University of Bayreuth
Bayreuth, Germany
renato.mio-zaldivar@uni-bayreuth.de

Jan Bodenschlägel
Chair of Digital Health & Data Science
University of Bayreuth
Bayreuth, Germany
jan.bodenschlaegel@uni-bayreuth.de

A. Aldo Faisal
Brain & Behaviour Lab
Imperial College London
London, UK
Chair of Digital Health & Data Science
University of Bayreuth
Bayreuth, Germany
aldo.faisal@uni-bayreuth.de

***Abstract*—Estimating muscle force production from neural drive is essential for advanced human-machine interfaces and understanding motor control. Although motor unit (MU) spike trains derived from high-density surface electromyography (HD-sEMG) have been used in gesture recognition and force estimation, the role of neural drive feature granularity (i.e. level of detail in its representation) in force regression remains understudied. In this study, we recorded HDsEMG of the anterior forearm from 25 participants performing isometric finger flexion and compare three sets of neural drive-derived features of increasing granularity: discharge rates (DRs) of ten representative MUs, DRs from two cumulative spike trains (CSTs) from 5 early and 5 late recruited MUs, and DRs from a single CST from all 10 MUs. These features were used to train regression models including linear models, XGBoost, multilayer perceptrons (MLPs), and recurrent neural networks (RNN, GRU, LSTM). Our results show that higher granularity of neural drive-derived features improves prediction, particularly in LSTM models, which achieved coefficient of determination values up to 0.944. Unlike prior subject- and task-specific approaches, the proposed pipeline generalises across participants and digits. These findings demonstrate that MU-level detail is crucial for accurate force regression and offer a foundation for generalisable MU-based neural interfaces.**

***Index Terms*—high-density EMG, motor unit decomposition, force prediction, finger force estimation, motor neurons.**

I. Introduction

The decoding of human motor intent from electromyography (EMG) has been a significant area of research, with applications ranging from prosthetic control to assistive and potentially commercial human-computer interfaces [1]–[3]. Many studies have focused on classifying hand gestures from EMG signals recorded using a few electrodes or high-density arrays. Recent advances have demonstrated the use of high-density surface EMG (HDsEMG) for effective gesture-based control of assistive devices and for recognising motion intent by combining hand kinematics with HDsEMG from forearm and far-field potentials [4], [5].

This work is supported by the Hightech-Agenda Bavaria. AAF acknowledges support from the United Kingdom Research and Innovation Turing AI Fellowship (EP/V025449/1).

Building on these EMG-based approaches, recent advances in motor unit (MU) decomposition that non-invasively decode individual motoneuron spike trains from HDsEMG have allowed the characterisation of populations of MUs and their behaviours related to muscle force and movement control [6], [7], also known as the neural drive to muscles. Moreover, the online implementation of MU decomposition holds the potential for novel neural interfaces that better exploit human neural bandwidth by interfacing with several spinal motoneurons recorded from each muscle [8], [9]. In particular, MU decomposition from the forearm muscles yields a high potential for gesture recognition and hand pose regression [2]. However, regression from MU spike trains and their discharge rates to variable forces remains understudied.

This presents several challenges. First, MU decomposition algorithms converge to a variable number of MUs across trials, and the specific MUs decoded can also vary, which makes MU drive-to force regression models unable to be trained on a stable set of input features. Second, the abrupt recruitment of MUs can cause sudden changes in their discharge rates, resulting in non-smooth input features. Third, while various methods have been used for MU-to-force regression [10]–[13], a systematic evaluation of different models or how much detail from the neural drive is necessary for optimal force representation has been lacking. A common approach involves using the cumulative spike train (CST) derived from an arbitrary number of MUs as input for force regression models, typically as a baseline for comparison. However, due to the variable number of MUs typically decoded per trial, approaches using individual MU discharge rates have primarily been limited to subject-specific or even subject-and-task-specific models, which constrains their broader applicability.

To address these limitations, in this study we collected a novel dataset from 25 participants, involving HDsEMG recordings from hand extrinsic muscles during finger flexion isometric contractions. We performed finger force regression using features derived from decomposed MU spike trains, systematically evaluating a range of machine learning models for regression from neural drive-derived features of varying

granularity. Here, feature granularity refers to the level of detail in the neural drive representation, from individual MU discharge rates (high granularity) to CSTs from multiple MUs (low granularity). We hypothesised that features representing a finer granularity of the neural drive would lead to improved prediction accuracy.

A key goal of this work is to establish a more robust method for dynamic finger force prediction by engineering neural features from decomposed HDsEMG that can generalise across subjects and tasks. The standardised pipeline approach presented here also has the potential to facilitate dataset pooling across different subjects, tasks, and muscles, which would enable the development of more complex models that could benefit from deep learning approaches.

II. Methods

A. Data collection

A custom finger force measurement device, similar in shape to a vertical computer mouse, was designed on Autodesk Inventor 2024 and then 3D-printed on an AnyCubic Kobra 3D printer and using polylactic acid filament (see Fig. 1a). The device was fitted with load cells with a 10 kg range, which allows recordings within the typical maximum isometric pinch forces of the targeted fingers [14], [15]. In addition, the device included Velcro straps to secure the hand and individual fingertips to the sensors. The output of the load cells was converted using a CJMCU-711 24-bit analog-digital converter and sent to an Arduino Uno R3. Force data were sampled at 50 Hz and sent from Arduino to the PC via serial communication.

The EMG recording setup comprised two 64-channel electrode grids with 5 rows x 13 columns topology and 8 mm inter-electrode distance (HD08MM1305, OT Bioelettronica, Turin, IT), totaling 128 monopolar channels placed over the anterior forearm (see Fig. 1b). Two Sessantaquatro (OT Bioelettronica, Italy) were used to amplify and sample HDsEMG at 2000 Hz (see Fig. 1c). When needed, the participant's forearm was shaved, cleaned, and prepared with abrasive gel. The electrode grids were attached using adhesive foams (FOA08MM1305, OT Bioelettronica, Turin, Italy) and the forearm was wrapped with an additional fixation bandage.

The task consisted in following a trapezium force trace (see Fig. 1d) by controlling finger forces applied over the sensors using the dominant hand. The force trace had a 5-second rest at the beginning and end, a 60-second plateau, and an ascending and descending slope of 5% of the participant's maximum voluntary force (MVF). Participants should perform the trials for each of the thumb, index and middle fingers and at two target forces of 10% and 20% of their individual maximum voluntary force, resulting in six distinct digit-force level conditions and with five repetitions per condition. The experimental protocol was approved by the Ethics Committee of the University of Bayreuth (Application No. 24-030).

B. Feature extraction

The complete pipeline followed for signal processing and feature extraction is shown in Fig. 2a. EMG trials were

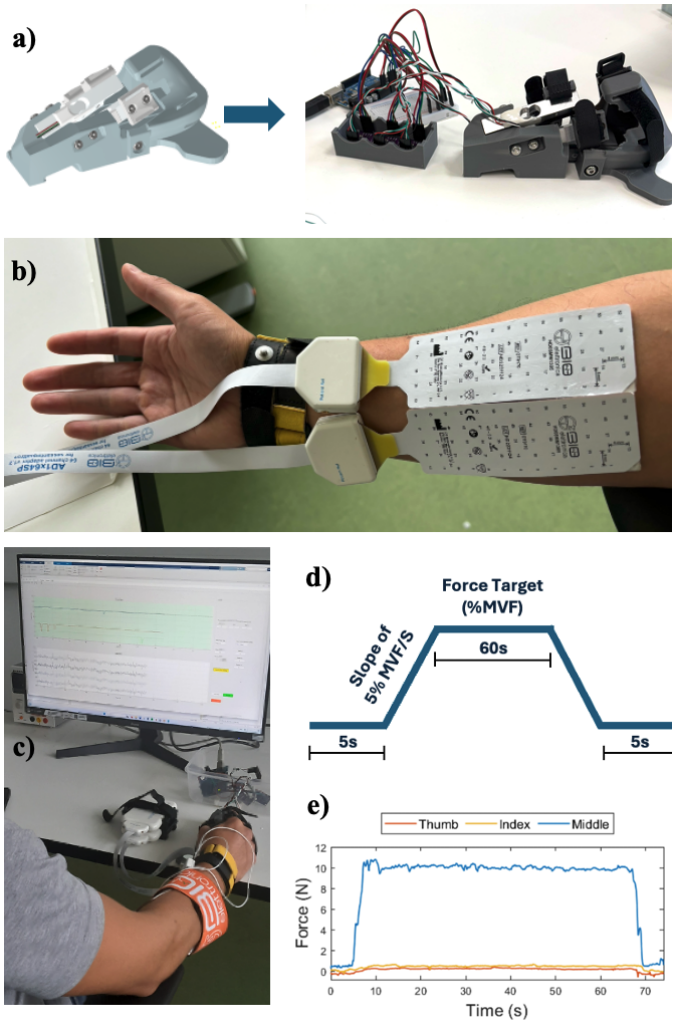

Fig. 1. Data collection setup. a) Custom finger force measurement device. b) High-density electrode grids over forearm flexors (128 channels). c) Matlab GUI showing the force trace visual stimulus. d) Trapezium force trace. e) Single trial force recording with middle finger as the target for control.

first preprocessed using a 4th order Butterworth bandpass filter between 20-500 Hz. Line interference was removed by applying a Notch filter at 50 Hz and its harmonics. EMG channels were then manually inspected for artifacts or high noise levels, and flat or noisy channels were removed. MU decomposition was then applied to the preprocessed trials using the convolutive kernel compensation (CKC) algorithm with peel-off [16], [17] for 100 iterations and a silhouette threshold of 0.7. The decomposition was applied separately to each electrode grid and then potential duplicates were removed by comparing the discharge times between all MUs across the grids and discarding those with over 30% matching spikes.

To standardise our pipeline, we further assessed the quality of the spike trains to retain only those that had potential to represent the neural drive controlling varying force. We removed all MUs with tonic behaviour (firing throughout the whole trial) or with MUs sparse activity (gaps in activity of over 1s) during the force-active segment. Finally, we only

kept trials that had at least 10 representative MUs, five early-recruited MUs and five late-recruited. We chose this number because 10 MUs have previously been shown to adequately represent neural drive [18] and because models would struggle with too few MUs known to have distinct non-linear rate coding in relation to applied force [7]. The early and late-recruited MU cohorts were defined as those MUs recruited at a force less than or equal to half of the maximum target force and those recruited at a force above half of the maximum target force, respectively. When more than five MUs per cohort met the criteria, the most active MUs as determined by their number of spikes were kept. This step ensured that there was a correlation over time between force activity and the activity of the selected MUs.

For our regression features derived from neural drive, we considered three different sets at different levels of granularity.

- Ten MUs, five early-recruited and five late-recruited, termed the "10MU" set (see Fig. 2d).
- Two cumulative spike trains, coming from the five early-recruited and the five late-recruited MUs, termed the "2CST" set (see Fig. 2e).
- One cumulative spike train from all ten MUs, termed the "1CST" set (see Fig. 2f).

Continuous discharge rates (DRs) were calculated for each feature spike train using a method derived from [19]. Support Vector Regression (SVR) models were fitted from individual MU spike trains with custom hyperparameters. For each MU, the regularisation and kernel scale hyperparameters were found after a grid search across 50-500 at increments of 10 and 0.5-5 at increments of 0.5 respectively. The grid search aimed to minimise the difference between the SVR estimation and the continuous DRs produced by using the more conventional approach of convolving the spike trains by a Hann window [20], [21]. The window used for this study was 1 second long.

The trial segment used for regression modelling focused on the initial force variation (see Fig. 2c), including the ramp-up phase and two adjacent segments of equal time length (one-third rest, one-third ramp-up, one-third constant plateau). This selection aimed to capture transient behaviours during force scaling and MU recruitment while maintaining a balanced dataset for these phases. Input features were generated using time windows ranging from 50 ms to 250 ms in 50 ms increments, with a 50% overlap between windows. The minimum window length was chosen based on typical MUAP waveform durations relevant for spike-triggered averaging (≈25 ms).

C. Regression models

We trained and compared the following regression models to predict finger force from the neural drive-derived features: Linear Regression, Ridge Regression, Generalised Additive Models (GAM), Generalised Linear Models (GLM), Multilayer Perceptron (MLP), XGBoost, Recurrent Neural Network (RNN) and its variants, Gated Recurrent Units (GRU) and Long Short-Term Memory (LSTM). Models were trained using 5-fold cross-validation, with performance averaged across folds. We used mean squared error (MSE) loss for training

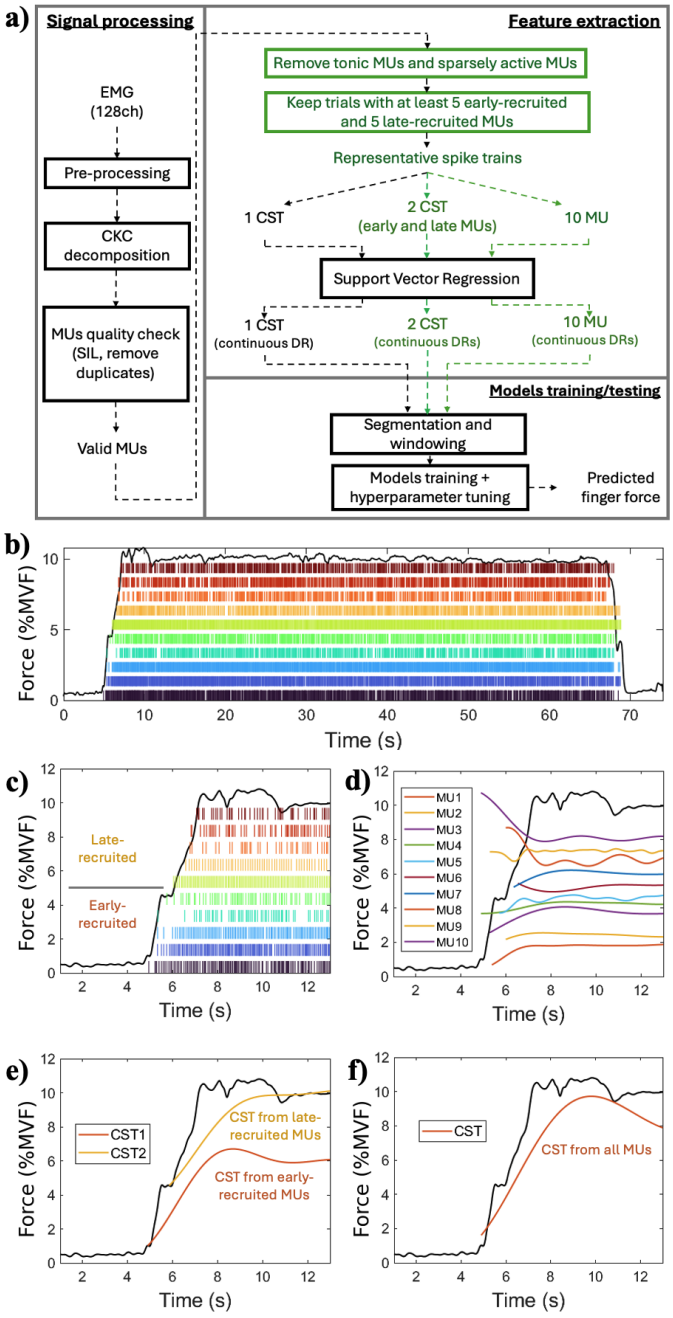

Fig. 2. Processing pipeline from HDsEMG to neural drive-derived features to predicted finger force. a) The steps for selection of motor neurons that better represent neural drive and engineering them as input features are highlighted in green. These steps make the resulting dataset and models subject- and task-independent. b) Single trial showing force trace (black) and 10 representative spike trains decomposed from HDsEMG. c) Ramp-up phase of the trial. d) 10MU feature set: Smoothed discharge rates from the 10 MUs. e) 2CST feature set: Smoothed discharge rates from two cumulative spike trains, coming from early and late recruited MUs respectively. f) 1CST feature: Smoothed discharge rate from the total cumulative spike train.

and report the coefficient of determination (R^2), mean absolute error (MAE), and root-mean-squared error (RMSE) as performance metrics.

Where applicable (i.e., for MLP, XGBoost, RNN-based models), a grid search was performed for hyperparameter

TABLE I
HYPERPARAMETERS PER MODEL AND INPUT FEATURE TYPE

Model name	Input features		
	10MU	***2CST***	***1CST***
MLP	hidden_dim: 64 batch_size: 16 lr: 1e-3	hidden_dim: 64 batch_size: 32 lr: 1e-3	hidden_dim: 64 batch_size: 16 lr: 1e-3
XGBoost	n_estimators: 50 max_depth: 3 lr: 0.1	n_estimators: 50 max_depth: 3 lr: 0.1	n_estimators: 50 max_depth: 3 lr: 0.1
RNN	hidden_dim: 128 num_layers: 1 batch_size: 32 lr: 1e-3	hidden_dim: 128 num_layers: 1 batch_size: 64 lr: 1e-3	hidden_dim: 128 num_layers: 1 batch_size: 32 lr: 1e-3
GRU	hidden_dim: 128 num_layers: 1 batch_size: 32 lr: 1e-3	hidden_dim: 128 num_layers: 2 batch_size: 64 lr: 1e-3	hidden_dim: 64 num_layers: 2 batch_size: 64 lr: 1e-3
LSTM	hidden_dim: 128 num_layers: 1 batch_size: 32 lr: 1e-3	hidden_dim: 128 num_layers: 1 batch_size: 64 lr: 1e-3	hidden_dim: 128 num_layers: 2 batch_size: 64 lr: 1e-3

lr: learning rate

tuning. The results presented consider the best-performing parameters for each model and input feature set, which are listed in Table I. The models were implemented primarily in the PyTorch framework and trained on a NVIDIA GeForce RTX 3080 GPU. For inference, to improve temporal resolution, a sliding window with a step size of 50 ms (equal to the smallest training window) was applied. Finally, a feature ablation experiment was performed in the three best models trained on the 10MU set. The experiment consisted of alternating random removal of MUs from the early and late-recruited cohorts, with the purpose of assessing how much the number of active inputs impacts the model performance. To do this, MUs were randomly masked alternating between cohorts and then the performance (R^2) was evaluated using the masked input feature matrix. The random MU removal procedure was started from 100 different random seeds.

III. RESULTS

We recruited 25 healthy participants (aged 28.8 ± 7.7 years, 15 female, 22 right-handed) without reported neuromotor pathologies. All participants gave written informed consent. After preprocessing and visual inspection of the EMG data, on average 6.5 $\pm$ 4.3 bad channels per trial were excluded.

The initial decomposition procedure and removal of duplicate MUs yielded on average 429.8 ± 158.4 MUs per participant and 7.2 ± 5.3 per trial. After applying the trial inclusion criteria, only 166 of a total of 750 recorded trials were included. Of these, the number of trials corresponding to thumb, index, and middle finger flexion were 52, 45, and 67, respectively. On average, 21.9$\pm$17.9% of trials were included per participant. Most of the discarded trials were due to particular participants with a low MU count yield after decomposition, which could arise from individual differences, as also seen in the inter-subject variabilities in previous work [22], [23]. The final sets of MU spike trains, coming from different subjects and task conditions, were then converted to continuous discharge rates, segmented, and windowed.

A. Model performance comparison

The systematic evaluation of the regression models revealed distinct performance characteristics based on the input feature granularity and model complexity. Fig. 3a and Fig. 3b summarise the performance of all models tested across the three neural feature sets: 10MU, 2CST, and 1CST.

Among all models tested, the LSTM model with the 10MU feature set achieved the highest performance, with an average R^2 value of approx. 0.925 across window sizes and folds, closely followed by the GRU model. In particular, the LSTM model with an input window length of 50 ms had the overall highest R^2 of 0.944, with minimum MAE of 1.24%MVF and minimum RMSE of 1.88 %MVF. While the R^2 is on par with subject-specific models from the literature, both the MAE and RMSE values obtained here outperform them [10]–[13]. Other models like MLP, XGBoost, and GAM also performed well with the 10MU feature set, although typically with lower R^2 values compared to the RNN variants. Linear models (MLR, Ridge) generally showed the lowest performance across all feature sets, highlighting the non-linear nature of the force-neural drive relationship.

Fig. 3c shows force prediction traces for a representative trial using the RNN, GRU, and LSTM models with the 10MU feature set. These plots demonstrate the models' capability to track the ramp-up and plateau phases of the isometric contraction. The GRU and LSTM models show a closer fit to the ground truth force compared to the vanilla RNN model. The predictions capture the dynamic increase in force, although deviations, more apparent in the RNN case, are present and could be attributed to the onsets of MU recruitment.

B. Feature granularity analysis

Generally, models trained with the 10MU feature set, representing the highest granularity of neural drive, consistently achieved the best performance across all model types. This pattern was most pronounced for complex models, particularly RNN-based architectures. When using features with coarser granularity (2CST and 1CST), the performance of RNN-based models was still strong but less distinctly superior. In the 2CST case, the best performing model was the LSTM with 250 ms window (R^2=0.825, MAE = 2.36%, RMSE = 3.35%), closely followed by GRU with 250 ms window (R^2=0.824, MAE = 2.36%, RMSE = 3.35%). Simpler models provided comparable performance, as in the case of XGBoost at 50 ms window (R^2=0.823, MAE = 2.39%, RMSE = 3.37%). In the 1CST case, model performances were close between GRU at 250 ms window (R^2=0.821, MAE = 2.43%, RMSE = 3.38%), LSTM at 250 ms window (R^2=0.820, MAE = 2.47%, RMSE = 3.39%), GAM at 200 ms window (R^2=0.820, MAE = 2.43%, RMSE = 3.40%) and XGBoost at 200 ms window (R^2=0.820, MAE = 2.44%, RMSE = 3.40%). These results consistently demonstrated that finer neural drive granularity resulted in greater model performance, particularly for more complex RNNs.

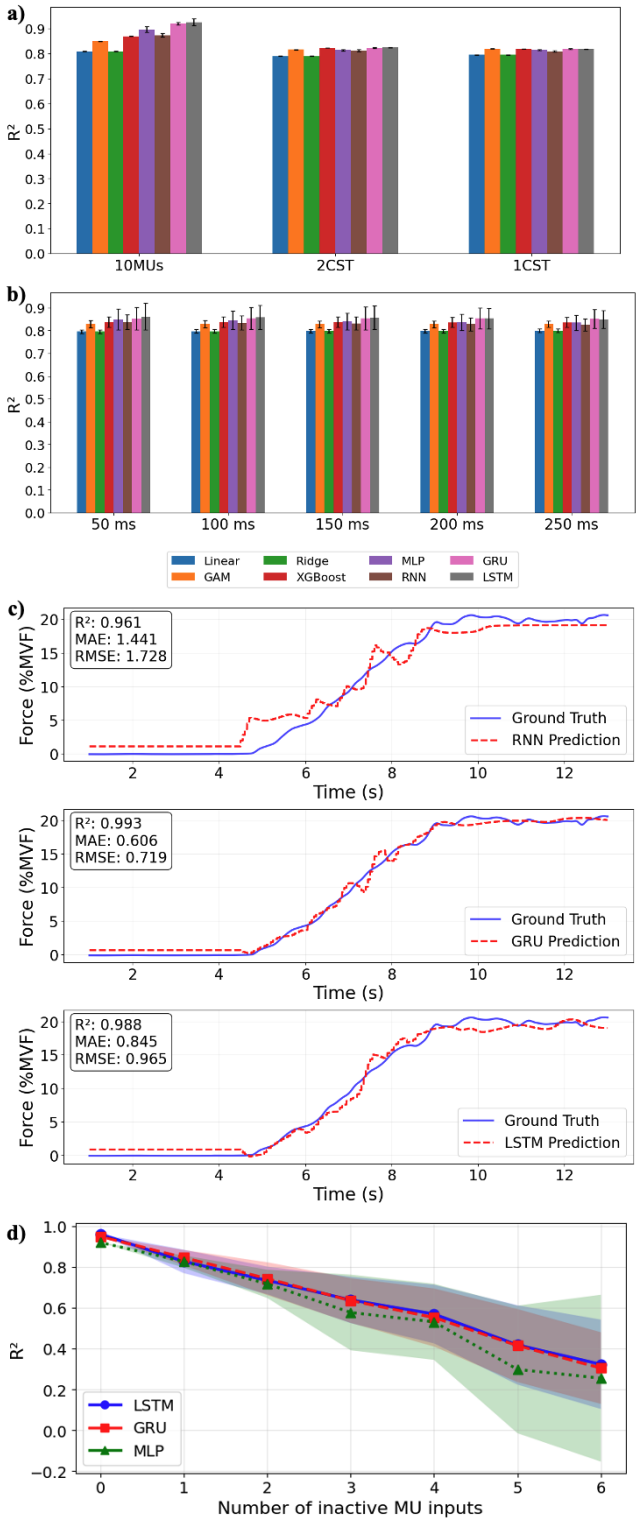

Fig. 3. (a) Model performance as a function of the input feature set. Error bars represent standard deviation across folds and window sizes. (b) Model performance as a function of the window used for training in ms. Error bars represent standard deviation across folds and type of input feature. (c) Performance of RNN-based models in predicting finger force for a trial of subject 9 with target force 20%MVF and the thumb finger. (d) Feature ablation results on the top three performing models. Shaded areas represent the standard deviation across 100 runs of MU random masking.

C. Feature ablation

Fig. 3d shows the results of the feature ablation experiment. The performance of models decreases monotonically as more MUs become inactive, with a collapse when 6 MUs are masked. The decrease followed a quasilinear pattern for both LSTM and GRU models, with standard deviations across runs also increasing linearly as more MUs became inactive. This suggests that individual MUs contribute similarly to model performance, and that maintaining a sufficient number of active MUs is critical for reliable force prediction.

IV. Discussion

This work systematically evaluated the impact of neural drive granularity and model complexity on finger force regression using neural drive-derived features. Our results demonstrate that detailed representations, specifically continuous DRs of 10 selected MUs, consistently yield higher prediction accuracy, particularly when combined with RNN architectures such as LSTM and GRU. This suggests that preserving individual MU firing behaviour is beneficial for accurately regressing variable force. Crucially, models trained on these features generalised well across subjects and tasks, despite the relatively small number of input MUs.

The performance gap between models was most pronounced with finer-grained input. LSTM networks significantly outperformed others with the 10MU feature set, potentially due to their ability to capture temporal dynamics in discharge patterns. In contrast, for coarser features such as single or dual CSTs, simpler models like XGBoost and GAM were competitive, sometimes outperforming more complex networks. This suggests that when input features are less detailed, additional model complexity may risk overfitting.

Our focus on the ramp-up phase of isometric contraction proved particularly informative, capturing MU recruitment and rate modulation processes that encode force scaling. The feature ablation experiment revealed that force decoding remained viable when few MUs were inactive, but degraded quasilinearly as the number of inactive MUs increased, suggesting similar importance across MUs for model performance.

Beyond model performance, our pipeline introduces a reproducible method for selecting early- and late-recruited MUs, standardising feature extraction and cross-subject data pooling. A significant implication of our pipeline is its potential for integrating heterogeneous HDsEMG datasets. Transforming multichannel EMG into MU spike trains shifts the focus from spatiotemporal patterns to temporal neural firings. This standardisation makes our approach robust to variations in electrode placement, enabling the pooling of data from different setups to build large-scale neural drive databases, which would in turn improve model robustness. Nonetheless, a drawback of our pipeline was the need for at least 10 input MUs, which resulted in many trials being discarded. Future work should focus on adapting the model to handle incomplete inputs, thus allowing all or most trials to meet the inclusion criteria.

However, integrating diverse datasets poses the challenge of negative transfer. This phenomenon, where combining

data from heterogeneous sources degrades performance, is a known challenge in brain-computer interfaces based on electroencephalography (EEG) and EMG [24]–[26]. It typically arises from differences in both electrode placement and the underlying task domains. Our approach addresses heterogeneity in electrode placement, by relying on temporal MU activity, but future work should investigate the benefits and challenges of including data from different tasks and muscles. Importantly, cross-participant generalisation in EMG-based neural interfaces has recently been demonstrated at large scale [3]. While their landmark work confirms the feasibility of building generic EMG interfaces, our results show that a complementary pathway towards generalisable neural interfaces exists at the level of MU activity.

V. Conclusion

This study demonstrates that finger force can be accurately predicted from MU spike trains, with finer-grained neural drive representations (10 MUs) yielding higher accuracy (R^2 up to 0.944) than coarser features, especially with LSTM models. Our standardised pipeline enables robust cross-subject generalisation, overcoming a key limitation of subject-specific approaches and providing clear evidence that preserving motor-unit level detail is crucial for accurate force regression

The pipeline's transformation of HDsEMG data into standardised MU-based features potentially enables integration of heterogeneous datasets from different electrode configurations and muscle groups into large-scale neural drive databases. This standardisation approach can extend beyond finger force prediction to other muscle groups and isometric contraction tasks. Future work should investigate domain adaptation techniques for enhanced generalisability across different datasets.

References

[1] M. Xiloyannis, C. Gavriel, A. A. C. Thomik, and A. A. Faisal, "Dynamic forward prediction for prosthetic hand control by integration of EMG, MMG and kinematic signals," in *2015 7th International IEEE/EMBS Conference on Neural Engineering (NER)*, 2015, pp. 611–614.

[2] R. C. Sîmpetru, D. I. Braun, A. U. Simon, M. März, V. Cnejevici, D. S. de Oliveira, N. Weber, J. Walter, J. Franke, D. Höglinger, C. Prahm, M. Ponfick, and A. D. Vecchio, "Myogestic: Emg interfacing framework for decoding multiple spared motor dimensions in individuals with neural lesions," *Science Advances*, vol. 11, no. 15, 2025.

[3] P. Kaifosh, T. R. Reardon, and CTRL-labs at Reality Labs, "A generic non-invasive neuromotor interface for human-computer interaction," *Nature*, Jul. 2025.

[4] J. Yang, K. Shibata, D. Weber, and Z. Erickson, "High-density electromyography for effective gesture-based control of physically assistive mobile manipulators," *npj Robotics*, vol. 3, no. 2, Jan 2025.

[5] I. M. Guerra, D. Y. Barsakcioglu, I. Vujaklija, D. Z. Wetmore, and D. Farina, "Far-field electric potentials provide access to the output from the spinal cord from wrist-mounted sensors," *Journal of Neural Engineering*, vol. 19, 4 2022.

[6] R. Mio, J. Narayan, and A. A. Faisal, "Motor unit decomposition over intrinsic hand muscles during single and multi-finger flexion," in *Emerging Therapies in Neurorehabilitation III*, J. L. Pons, D. Farina, and J. Tornero, Eds. Cham: Springer Nature Switzerland, 2025, pp. 115–119.

[7] S. Avrillon, F. Hug, R. M. Enoka, A. H. Caillet, and D. Farina, "The identification of extensive samples of motor units in human muscles reveals diverse effects of neuromodulatory inputs on the rate coding," *eLife*, vol. 13, p. RP97085, Dec 2024.

[8] J. Rossato, F. Hug, K. Tucker, C. Gibbs, L. Lacourpaille, D. Farina, and S. Avrillon, "I-spin live, an open-source software based on blind-source separation for real-time decoding of motor unit activity in humans," *eLife*, vol. 12, 10 2024.

[9] J. Rossato, S. Avrillon, K. Tucker, D. Farina, and F. Hug, "The volitional control of individual motor units is constrained within low-dimensional neural manifolds by common inputs," *Journal of Neuroscience*, vol. 44, no. 34, 2024.

[10] N. Rubin, Y. Zheng, H. Huang, and X. Hu, "Finger force estimation using motor unit discharges across forearm postures," *IEEE Transactions on Biomedical Engineering*, vol. 69, pp. 2767–2775, 9 2022.

[11] H. Zhao, Y. Sun, C. Wei, Y. Xia, P. Zhou, and X. Zhang, "Online prediction of sustained muscle force from individual motor unit activities using adaptive surface EMG decomposition," *Journal of NeuroEngineering and Rehabilitation*, vol. 21, 12 2024.

[12] W. Guo, Z. Zhao, Z. Zhou, Y. Fang, Y. Yu, and X. Sheng, "Hand kinematics, high-density semg comprising forearm and far-field potentials for motion intent recognition," *Scientific Data*, vol. 12, 12 2025.

[13] M. Montazerin, E. Rahimian, F. Naderkhani, S. F. Atashzar, S. Yanushkevich, and A. Mohammadi, "Transformer-based hand gesture recognition from instantaneous to fused neural decomposition of high-density emg signals," *Scientific Reports*, vol. 13, 12 2023.

[14] H. Kinoshita, T. Murase, and T. Bandou, "Grip posture and forces during holding cylindrical objects with circular grips," *Ergonomics*, vol. 39, no. 9, pp. 1163–1176, 1996.

[15] Y. Li, N. Lv, Y. Zhao, Z. Wang, C. Xue, and X. Hao, "Contributions of the thumb and index finger to tip pinch force sense," *Scientific Reports*, vol. 15, no. 23687, 2025.

[16] F. Negro, S. Muceli, A. M. Castronovo, A. Holobar, and D. Farina, "Multi-channel intramuscular and surface emg decomposition by convolutive blind source separation," *Journal of Neural Engineering*, vol. 13, 2 2016.

[17] M. Chen and P. Zhou, "A novel framework based on FastICA for high density surface EMG decomposition," *IEEE Transactions on Neural Systems and Rehabilitation Engineering*, vol. 24, pp. 117–127, 1 2016.

[18] D. Farina, F. Negro, and J. L. Dideriksen, "The effective neural drive to muscles is the common synaptic input to motor neurons," *The Journal of Physiology*, vol. 592, no. 16, pp. 3427–3441, 2014.

[19] J. A. Beauchamp, O. U. Khurram, J. P. Dewald, C. J. Heckman, and G. E. Pearcey, "A computational approach for generating continuous estimates of motor unit discharge rates and visualizing population discharge characteristics," *Journal of Neural Engineering*, vol. 19, 2 2022.

[20] A. S. Hassan, M. E. Fajardo, M. Cummings, L. M. McPherson, F. Negro, J. P. A. Dewald, C. J. Heckman, and G. E. P. Pearcey, "Estimates of persistent inward currents are reduced in upper limb motor units of older adults," *The Journal of Physiology*, vol. 599, no. 21, pp. 4865–4882, 2021.

[21] Y. Wen, S. J. Kim, S. Avrillon, J. T. Levine, F. Hug, and J. L. Pons, "A Deep CNN Framework for Neural Drive Estimation From HD-EMG Across Contraction Intensities and Joint Angles," *IEEE Transactions on Neural Systems and Rehabilitation Engineering*, vol. 30, pp. 2950–2959, 2022.

[22] D. S. d. Oliveira, A. Casolo, T. G. Balshaw, S. Maeo, M. B. Lanza, N. R. W. Martin, N. Maffulli, T. M. Kinfe, B. M. Eskofier, J. P. Folland, D. Farina, and A. Del Vecchio, "Neural decoding from surface high-density EMG signals: influence of anatomy and synchronization on the number of identified motor units," *J. Neural Eng.*, vol. 19, no. 4, Aug. 2022.

[23] C. A. Taylor, B. H. Kopicko, F. Negro, and C. K. Thompson, "Sex differences in the detection of motor unit action potentials identified using high-density surface electromyography," *J. Electromyogr. Kinesiol.*, vol. 65, no. 102675, Jun. 2022.

[24] X. Wei, J. Narayan, and A. A. Faisal, "The 'Sandwich' meta-framework for architecture agnostic deep privacy-preserving transfer learning for non-invasive brainwave decoding," *Journal of Neural Engineering*, vol. 22, no. 1, p. 016014, Jan 2025.

[25] X. Wei, P. Ortega, and A. A. Faisal, "Inter-subject Deep Transfer Learning for Motor Imagery EEG Decoding," in *2021 10th International IEEE/EMBS Conference on Neural Engineering (NER)*, 2021, pp. 21–24.

[26] J. Han, X. Wei, and A. A. Faisal, "EEG decoding for datasets with heterogenous electrode configurations using transfer learning graph neural networks," *Journal of Neural Engineering*, vol. 20, no. 6, p. 066027, Dec 2023.